AS6320

Assignment 3:

Thermoacoustic Interactions in Rijke Tube

Pavan Kumar G

AE20B042

(Dated: 13 May 2023)

In this study, we replicate and investigate the thermoacoustic interactions in a Rijke tube. The heat release rate of the heating element is modeled using a modified form of King's law, treating the fluctuating heat release as a compact source in a one-dimensional linear acoustic field. By employing the Galerkin technique, we study the temporal evolution of acoustic perturbations. We find that thermoacoustic systems exhibit non-normal behavior, leading to algebraic growth of oscillations for a short duration. The findings contribute to understanding thermoacoustic dynamics and provide valuable insights for the design and stability of thermoacoustic systems in combustion and acoustics research.

I. INTRODUCTION

The Rijke tube, named after the Dutch physicist Petrus Leonardus Rijke, is a fundamental experimental apparatus used in the study of thermoacoustic phenomena. It serves as a simplified model to investigate the interaction between flames and acoustic waves in combustion systems. The unique design of the Rijke tube enables the observation and analysis of self-excited oscillations and their underlying mechanisms, making it a valuable tool for understanding and controlling thermoacoustic instabilities.

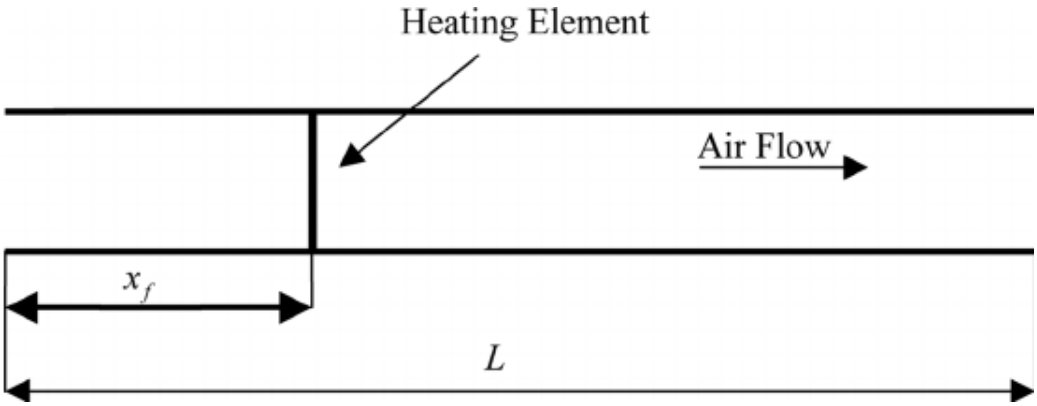

FIG. 1. Schematic of Horizontal Rijke Tube Setup

The Rijke tube consists of a closed-ended tube with a flame at one end and an open end at the other. The flame acts as a heat source, generating periodic temperature fluctuations and creating a coupling between the acoustic pressure oscillations and the heat release process. When certain conditions are met, such as specific flame characteristics and tube dimensions, a self-sustained oscillation known as a thermoacoustic instability occurs. However, for the purpose of the study we use heating wire element.

Thermoacoustic instabilities in the Rijke tube arise from the coupling between the unsteady heat release from the flame and the acoustic field. These instabilities can lead to undesirable effects, such as pressure fluctuations, flame flickering, and even catastrophic failure of combustion systems. Understanding the underlying mechanisms of thermoacous-

tic instabilities is crucial for designing efficient and stable combustion devices, such as gas turbines, rocket engines, and industrial furnaces.

By adopting a modified form of King's law to model the heat release rate of the heating element and using the Galerkin technique to study the temporal evolution of acoustic perturbations, we investigate the transient behavior and stability characteristics of the system. Our findings contribute to the broader understanding of thermoacoustic dynamics and provide valuable insights for the design and control of stable and efficient thermoacoustic systems.

The Runge-Kutta method is a popular numerical method for solving differential equations that offers high accuracy and stability for a wide range of problems. This method involves discretizing the differential equation into a set of algebraic equations, which are then solved iteratively to obtain the numerical solution. In this paper, we use this numerical method to solve equations of the Rijke tube model.

II. MODEL FOR RIJKE TUBE

As presented in the paper by Balasubramaniam and Sujith, the model involves neglecting the impact of mean flow and mean temperature gradient within the duct, and deriving the governing equations for the one-dimensional acoustic field.

$$\gamma M \frac{\partial u'}{\partial t} + \frac{\partial p'}{\partial x} = 0 \tag{1}$$

$$\frac{\partial p'}{\partial t} + \gamma M \frac{\partial u'}{\partial x} + \xi p' = (\gamma - 1)\dot{Q}'(t)\delta(x - x_f) \tag{2}$$

These are non dimensional linearized momentum and energy equations respectively. Here, $x = \tilde{x}/l$; $t = c_0/l\tilde{t}$; $u' = \tilde{u'}/u_0$; $p' = \tilde{p'}/\bar{p}$; $M = u_0/c_0$. x is the distance along the axial direction, l is the length of the duct and t is time. The steady state flow velocity, pressure, temperature, are u_0, $\bar{p}$ and temperature $\bar{T}$, and u' and p' are the acoustic velocity and pressure fluctuations.

Now we use the modified version(correction provided by Heckl) of the King's law that quantifies the heat release from the heating wire element given by

$$\dot{Q}'(t) = \frac{2L_w(T_w - \bar{T})}{S\sqrt{3}c_0\bar{p}}\sqrt{\pi\lambda C_V u_0 \bar{\rho} l_c}\left[\sqrt{\left|\frac{1}{3} + u'_f(t-\tau)\right|} - \sqrt{\frac{1}{3}}\right] \tag{3}$$

The energy equation by including the heat release rate term is given by:

$$\frac{\partial p'}{\partial t} + \gamma M\frac{\partial u'}{\partial x} + \xi p' = (\gamma - 1)\frac{2L_w(T_w - \bar{T})}{S\sqrt{3}c_0\bar{p}}\sqrt{\pi\lambda C_V u_0 \bar{\rho} l_c}\left[\sqrt{\left|\frac{1}{3} + u'_f(t-\tau)\right|} - \sqrt{\frac{1}{3}}\right]\delta(x - x_f) \tag{4}$$

Here, γ is the heat capacity ratio, L_w and l_c refer to the equivalent length and diameter of the wire, $(T_w - \bar{T})$ is the temperature difference between the wire and the ambient temperature, S is the cross-sectional area of the duct, λ, C_V, u_0 are the heat conductivity, the specific heat of air at constant volume, and the mean velocity of the air, respectively. τ is the time lag accounting for the thermal inertia of the medium and u_f is the velocity fluctuations at the location of heater mesh. ξ is the damping coefficient.

Note that, quantities with tilde are dimensional and those without tilde are non-dimensional.

To solve the equations we make use of the Galerkin Technique. It is a powerful mathematical method commonly used in solving partial differential equations. It involves representing the unknown variables, in this case, the acoustic perturbations, as a series of basis functions. These basis functions are typically chosen to be orthogonal or satisfy certain orthogonality properties. By projecting the governing equations onto these basis functions and applying the principle of weighted residuals, we obtain a system of ordinary differential equations that can be solved numerically. In the following expressions, $k_j = j\pi$ is the non-dimensional wave number and $\omega_j = j\pi$ is the non-dimensional angular frequency of the j^{th} duct mode.

$$u' = \sum_{j=1}^{\infty} U_j(t) cos(k_j x) \tag{5}$$

$$p' = \sum_{j=1}^{\infty} \frac{\gamma M}{j\pi} P_j(t) sin(k_j x) \tag{6}$$

$$\dot{U}_j + k_j P_j = 0 \tag{7}$$

$$\dot{P}_j + 2\xi\,\omega_j P_j - k_j U_j = K\left[\sqrt{\left|\frac{1}{3} + u'_f(t-\tau)\right|} - \sqrt{\frac{1}{3}}\right]\sin(x - x_f) \tag{8}$$

The heater power equation in the non-dimensional form from the above expression is given by,

$$K = (\gamma - 1)\frac{4L_w(T_w - \bar{T})}{\gamma M S\sqrt{3}c_0\bar{p}}\sqrt{\pi\lambda C_V u_0 \bar{\rho} l_c} \tag{9}$$

K is an important parameter, and is the main control parameter in the following simulation.

Also, $\xi = 2\omega_j\xi_j$ is the frequency dependent damping, where ξ_j is given by:

$$\xi_j = \frac{1}{2\pi}\left(c_1\frac{\omega_j}{\omega_1} + c_2\sqrt{\frac{\omega_1}{\omega_j}}\right) \tag{10}$$

III. RESULTS

Using the 2 sets of initial conditions i.e. for 2 values of non dimensional heater power (K), we plot the graphs for the variation of u' and acoustic energy with time.

The plots showing the above said variations for K=0.0004 are shown below:

The first plot shows the variation of acoustic velocity fluctuation vs time.

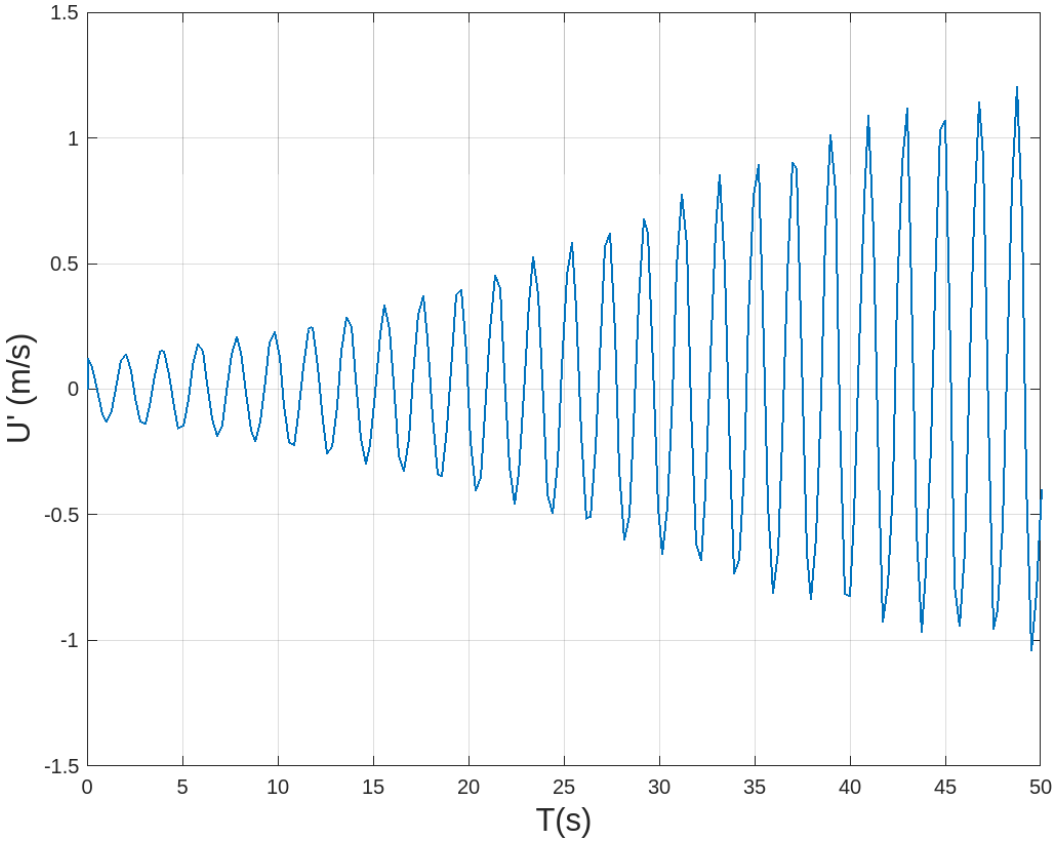

FIG. 2. Acoustic Velocity Fluctuation vs Time, K=0.0004

The second plot shows the variation of acoustic energy vs time.

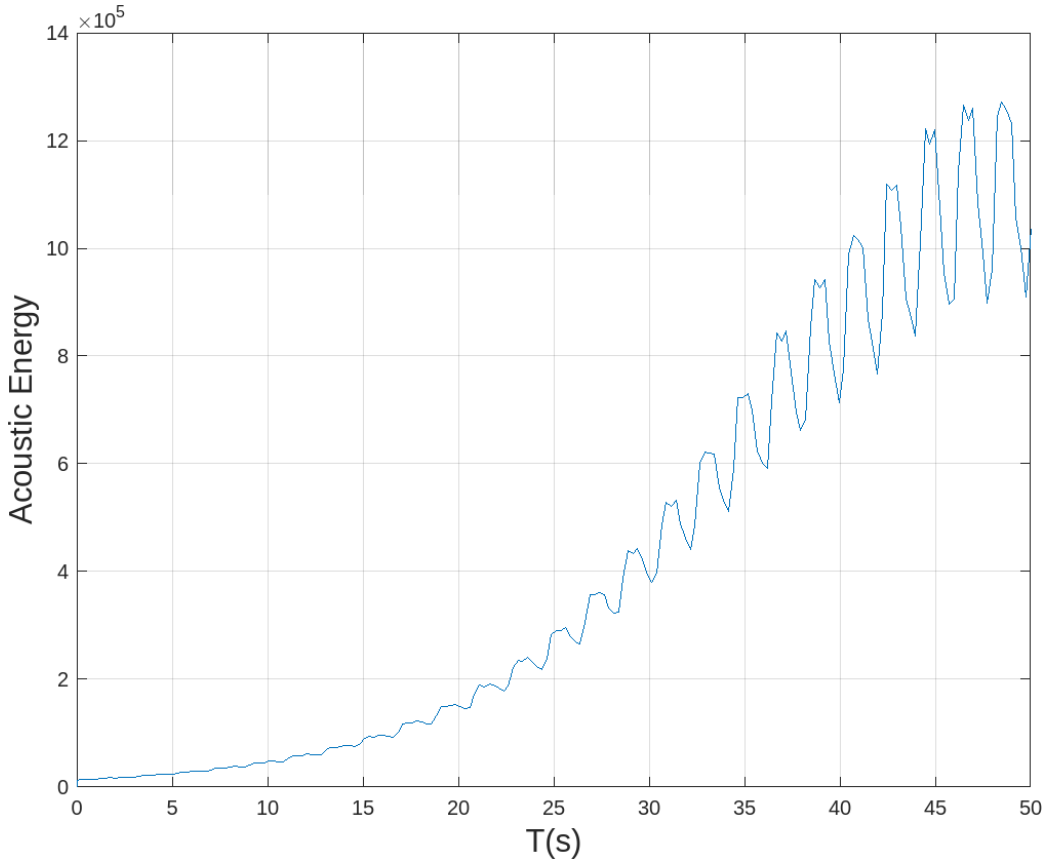

FIG. 3. Acoustic Energy vs Time, K=0.0004

The plots showing the above said variations for K=0.0001 are shown below:

The first plot shows the variation of acoustic velocity fluctuation vs time.

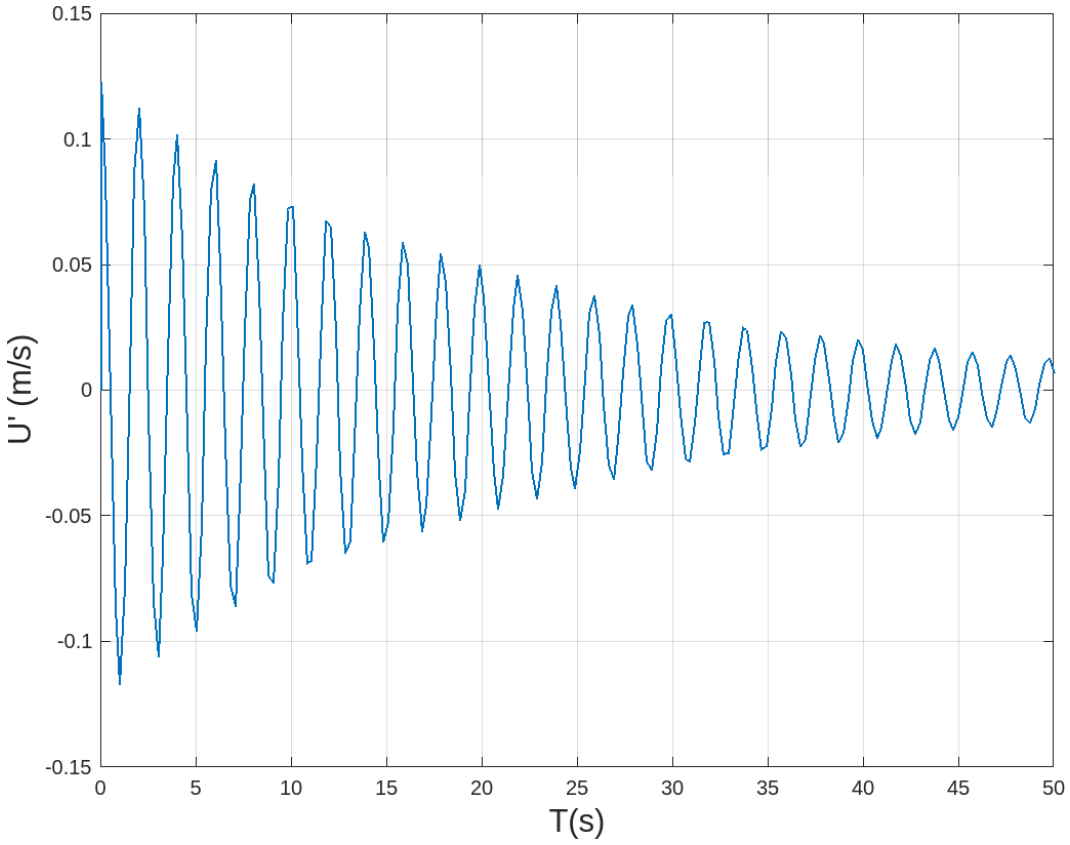

FIG. 4. Acoustic Velocity Fluctuation vs Time, K=0.0001

The second plot shows the variation of acoustic energy vs time.

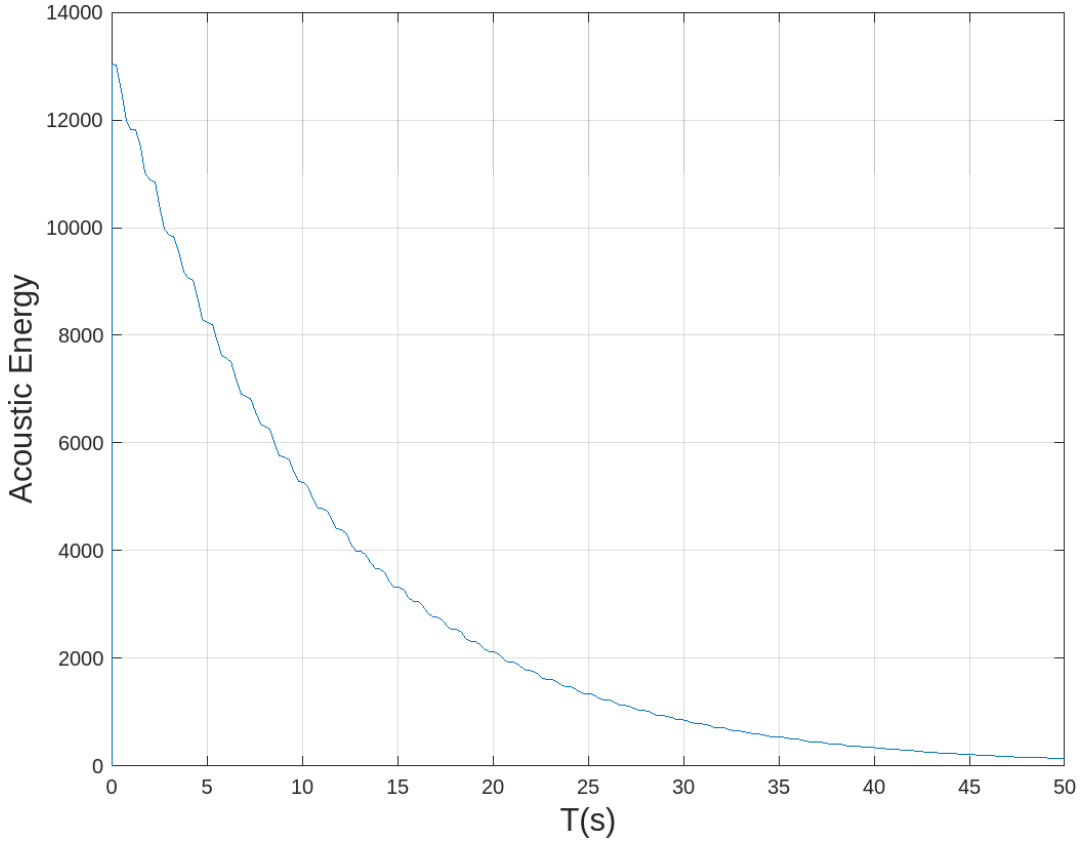

FIG. 5. Acoustic Energy vs Time, K=0.0001

We also see the bifurcation plot (|u'| vs K) obtained from varying the value of K from 0.0003 to 0.0009. The bifurcation for plot for the same values of K but with initial conditions being the end conditions of the first bifurcation plot is also plotted.

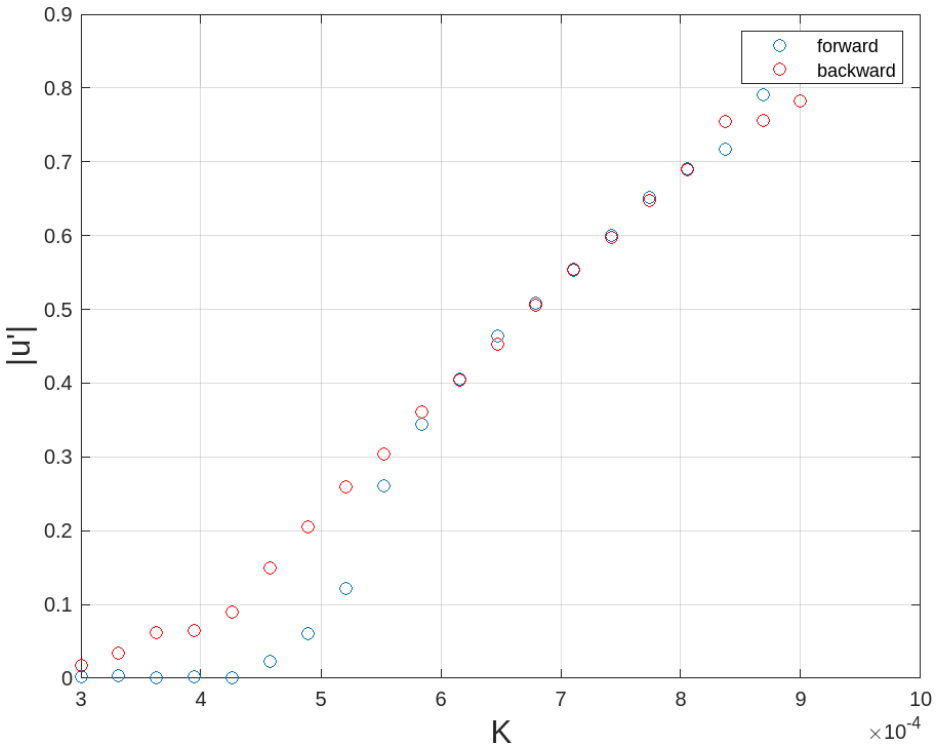

FIG. 6. Bifurcation Plot showing hysteresis

IV. INFERENCES

We see that the in the first set of plots for K= 0.0004, i.e. Fig 2 and Fig 3, the velocity fluctuation is increasing with time and so does the acoustic energy. However, in the last few seconds of the simulation it appears to saturate to a maximum value. In which case the heat release rate, which is the driving entity behind oscillations is matching the damping term hence neutralising each others' effect in those last few seconds. This is the stable limit cycle oscillations in the context of complex dynamical systems theory.

In the second set of plots, i.e. Fig 4 and Fig 5, both velocity fluctuations and the acoustic energy decreasing from a maximum value, which shows that the damping factor is dominant since the start and the driving force, in this case the heat release rate is unable to compensate for the damping. Thus the oscillations will approach zero at some large time.

In the last plot, which shows the bifurcation, we notice the presence of hysteresis. We see that the forward bifurcation plot has an abrupt increase followed by which it is again followed by a gradual increase. Hence this is a subcritical hopf bifurcation. The same is true for the backward bifurcation plot Since the path taken by the forward and backward bifurcation is different, it proves the presence of hysteresis.

V. CONCLUSION

Thus the above discussed method for modelling the oscillations in a horizontal Rijke tube led on to show the presence of bifurcation and presence of hysteresis.Overall, the Rijke tube serves as an essential experimental platform for studying thermoacoustic phenomena, offering a controlled environment to analyze the complex coupling between flames and acoustics. By advancing our knowledge of these interactions, we can enhance the understanding and management of thermoacoustic instabilities, ultimately leading to improved combustion system designs with enhanced efficiency and stability.

Appendix A: Codes used for generating the plots

The code for velocity and energy plots is attached below:

```
clear all;
close all;
clc;
Bnn=zeros(20,10);
bnl=zeros(20,10);
X0=zeros(20,1);
X0(1,1)=0.20;u0=0.5;
r=1.4;c0=399.6;
dw=0.0011;Ktbar=397;
K=0.0004;xf=0.29;
tau=0.45;w=@(J) J*pi;
Beta=@(J) sqrt(3)/(r*u0/c0)*K*J*pi*sin(J*pi*xf);
A1=zeros(20,20);
A2=zeros(20,20);
A3=zeros(20,20);
Bm=zeros(20,1);
Um=zeros(20,1);
Pm=zeros(20,1);

%%%%%%%%%%%%%%%%%%%%%%%%%%%%%%%%%%%%%%%%%%%%%%%%%%%%%%%%%%%%%%%%%%%%%%%%%%%%%

J=1;j=2;
for i=1:2:20
    Um(i,1)=cos(J*pi*xf);
    A1(i,j)=-1;
```

```
    j=j+2;J=J+1;
end
J=1;j=1;
for i=2:2:20
    Pm(i,1)=cos(J*pi*xf);
    Bm(i,1)=-Beta(J);
    A1(i,j)=(w(J)^2);
    j=j+2;J=J+1;
end
c1=0.1;c2=0.06;
zeta=@(J) (c1*(w(J)/pi)+c2*sqrt(pi/w(J)))/(2*pi);
j=2;J=1;
for i=2:2:20
    A1(i,j)=2*J*pi*zeta(J);
    J=J+1;j=j+2;
end
A2=Bm*Um';
A3=Bm*Pm';
Bnn=A1-A2+tau.*A3;
u=[];u(1)=0;
i=2;Xi=X0;
T=[];T(1)=0;
for t=linspace(0.01,50,200)
    T(i)=t;
    X=rk4(tau,Bnn,T(i),T(i-1),0.001,Xi,A2,A3,Um,Pm);
    sumu=0;sume=0;sump=0;
    Xi=X;
    n1(i)=X(1,1);
```

```
    n2(i)=X(3,1);
    J=1;M=2;m=1;
    for n=1:1:10
        sumu=sumu+X(m)*cos(n*pi*xf);
        sume=sume+(X(m)^2+(X(M)^2/(J*pi)^2));
        sump=sump+(-1.4*u0/(c0*J*pi)*X(M)*sin(J*pi*xf));
        J=J+1;M=M+2;m=m+2;
    end
    ea(i)=(0.5*sump^2+0.5*(1.4*u0*sumu/c0)^2)/(1.4*(u0)/c0)^2;
    u(i)=sumu;
    p(i)=sump;
    e(i)=sume/(1.4*(u0)/c0)^2;
    i=i+1;
end

%%%%%%%%%%%%%%%%%%%%%%%%%%%%%%%%%%%%%%%%%%%%%%%%%%%%%%%%%%%%%%%%%%%%%%%%%%%%%%%%

figure(1);
plot(T,u,LineWidth=1);
xlabel('T(s)',FontSize=15);
ylabel("U' (m/s)",FontSize=15);
grid on;
figure(2);
plot(T,n1,LineWidth=1);
xlabel('T(s)',FontSize=15);
ylabel('N_1',FontSize=15);
grid on;
figure(3);
```

```
plot(T,n2,LineWidth=1);
xlabel('T(s)',FontSize=15);
ylabel('N_2',FontSize=15);
grid on;
figure(4);
plot(T,e);
xlabel('T(s)',FontSize=15);
ylabel('Acoustic Energy',FontSize=15);
grid on;

%%%%%%%%%%%%%%%%%%%%%%%%%%%%%%%%%%%%%%%%%%%%%%%%%%%%%%%%%%%%%%%%%%%%%%%%%%%%%%

function Xs=rk4(tau,Bnn,T,to,h,x0,A2,A3,Um,Pm)
if((T-tau)<0)
    Udtua= @(X) Um'*X-tau.*Pm'*X;
    f=@(t,X) -Bnn*X;
end
if((T-tau)>=0)
    Udtua=@(X) Um'*X-tau.*Pm'*X;
    Bnl=@(X) 3/4.*Udtua(x0).*A2-3/4*tau.*Udtua(x0).*A3;
    f=@(t,X) -Bnn*X-Bnl(X)*X;
end
n=(T-to)/h;
for i=1:n
    k1=f(to,x0);
    k2=f(to+h/2,x0+0.5.*h.*k1);
    k3=f(to+h/2,x0+0.5.*h.*k2);
    k4=f(to+h,x0+h.*k3);
```

```
    k=(h/6).*(k1+2.*k2+2.*k3+k4);
    Xs=x0+k;
    x0=Xs;
    U=Udtua(Xs);
    to=to+h;
end
end
```

The code for bifurcation plot is attached here:

```
clear all;
close all
clc;
Bnn=zeros(20,20);
bnl=zeros(20,20);
X0=zeros(20,1);
X0(1,1)=0.20;
u0=0.5; r=1.4;
c0=399.6;
K_b = linspace(0.0003,0.0009,20);
for zz = 1:length(K_b)
    K = K_b(zz);
    xf=0.29;tau=0.45;
    w=@(J) J*pi;
    Beta=@(J) sqrt(3)/(r*u0/c0)*K*J*pi*sin(J*pi*xf);
    A1=zeros(20,20);
    A2=zeros(20,20);
```

```
A3=zeros(20,20);
Bm=zeros(20,1);
Um=zeros(20,1);
Pm=zeros(20,1);
J=1;j=2;
for i=1:2:20
    Um(i,1)=cos(J*pi*xf);
    A1(i,j)=-1;
    j=j+2;J=J+1;
end
J=1;j=1;
for i=2:2:20
    Pm(i,1)=cos(J*pi*xf);
    Bm(i,1)=-Beta(J);
    A1(i,j)=(w(J)^2);
    j=j+2;J=J+1;
end
c1=0.23;
c2=0.06;
zeta=@(J)(c1*(w(J)/pi)+c2*sqrt(pi/w(J)))/(2*pi);
j=2;J=1;
for i=2:2:20
    A1(i,j)=2*J*pi*zeta(J);
    J=J+1;j=j+2;
end
A2=Bm*Um';
A3=Bm*Pm';
Bnn=A1-A2+tau.*A3;
```

```
    u=[];u(1)=0;
    i=2;Xi=X0;
    T=[];T(1)=0;
    for t=linspace(0.01,50,200)
        T(i)=t;
        X=rk4(tau,Bnn,T(i),T(i-1),0.001,Xi,A2,A3,Um,Pm);
        sumu=0;sume=0;sump=0;
        Xi=X;
        n1(i)=X(1,1);
        n2(i)=X(3,1);
        J=1;M=2;m=1;
        for n=1:1:10
            sumu=sumu+X(m)*cos(n*pi*xf);
            sume=sume+(X(m)^2+(X(M)^2/(J*pi)^2));
            sump=sump+(-1.4*u0/(c0*J*pi)*X(M)*sin(J*pi*xf));
            J=J+1;M=M+2;m=m+2;
        end
        ea(i)=(0.5*sump^2+0.5*(1.4*u0*sumu/c0)^2)/(1.4*(u0)/c0)^2;
        u(i)=sumu;
        p(i)=sump;
        e(i)=sume;
        i=i+1;
    end
    R = n1(150:200);
    rr(zz) = max(R) - abs(min(R));
end
plot(K_b,rr,'o');
ylabel("|u'|",FontSize=15);
```

```
xlabel('K',FontSize=15);
grid on
legend({'forward'})
hold on
%%%%%%%%%%%%%%%%%%%%%%%%%%%%%%%%%%%%%%%%%%%%%%%%%%%%%%%%%%%%%%%%%%%%%%%%%%%%%%%%%%%%
clear
Bnn=zeros(20,20);
bnl=zeros(20,20);
X0=zeros(20,1);
X0(1,1)=2.01;
u0=0.5;r=1.4;
c0=399.6;
K_b = linspace(0.0009,0.0003,20)
for zz = 1:length(K_b)
    K = K_b(zz);
    xf=0.29;tau=0.45;
    w=@(J) J*pi;
    Beta=@(J) sqrt(3)/(r*u0/c0)*K*J*pi*sin(J*pi*xf);
    A1=zeros(20,20);
    A2=zeros(20,20);
    A3=zeros(20,20);
    Bm=zeros(20,1);
    Um=zeros(20,1);
    Pm=zeros(20,1);
    J=1;j=2;
    for i=1:2:20
        Um(i,1)=cos(J*pi*xf);
        A1(i,j)=-1;
```

```
    j=j+2;J=J+1;
end
J=1;j=1;
for i=2:2:20
    Pm(i,1)=cos(J*pi*xf);
    Bm(i,1)=-Beta(J);
    A1(i,j)=(w(J)^2);
    j=j+2;J=J+1;
end
c1=0.23;
c2=0.06;
zeta=@(J)(c1*(w(J)/pi)+c2*sqrt(pi/w(J)))/(2*pi);
j=2;J=1;
for i=2:2:20
    A1(i,j)=2*J*pi*zeta(J);
    J=J+1;j=j+2;
end
A2=Bm*Um';
A3=Bm*Pm';
Bnn=A1-A2+tau.*A3;
u=[];u(1)=0;
i=2;Xi=X0;
T=[];T(1)=0;
for t=linspace(0.01,50,200)
    T(i)=t;
    X=rk4(tau,Bnn,T(i),T(i-1),0.001,Xi,A2,A3,Um,Pm);
    sumu=0;sume=0;sump=0;
    Xi=X;
```

```
        n1(i)=X(1,1);
        n2(i)=X(3,1);
        J=1;M=2;m=1;
        for n=1:1:10
            sumu=sumu+X(m)*cos(n*pi*xf);
            sume=sume+(X(m)^2+(X(M)^2/(J*pi)^2));
            sump=sump+(-1.4*u0/(c0*J*pi)*X(M)*sin(J*pi*xf));
            J=J+1;
            M=M+2;
            m=m+2;
        end
        ea(i)=(0.5*sump^2+0.5*(1.4*u0*sumu/c0)^2)/(1.4*(u0)/c0)^2;
        u(i)=sumu;
        p(i)=sump;
        e(i)=sume;
        i=i+1;
    end
    R = n1(150:200);
    rr(zz) = max(R) - abs(min(R));
end
plot(K_b,rr,'ro');
legend({'forward','backward'})
%%%%%%%%%%%%%%%%%%%%%%%%%%%%%%%%%%%%%%%%%%%%%%%%%%%%%%%%%%%%%%%%%%%%%%%%%%%%%%%%%%%%
function Xs=rk4(tau,Bnn,T,to,h,x0,A2,A3,Um,Pm)
if((T-tau)<0)
    Udtua= @(X) Um'*X-tau.*Pm'*X;
    f=@(t,X) -Bnn*X;
end
```

```
if((T-tau)>=0)
    Udtua=@(X) Um'*X-tau.*Pm'*X;
    Bnl=@(X) 3/4.*Udtua(x0).*A2-3/4*tau.*Udtua(x0).*A3;
    f=@(t,X) -Bnn*X-Bnl(X)*X;
end
n=(T-to)/h;
for i=1:n
    k1=f(to,x0);
    k2=f(to+h/2,x0+0.5.*h.*k1);
    k3=f(to+h/2,x0+0.5.*h.*k2);
    k4=f(to+h,x0+h.*k3);
    k=(h/6).*(k1+2.*k2+2.*k3+k4);
    Xs=x0+k;
    x0=Xs;
    U=Udtua(Xs);
    to=to+h;
end
end
```

The plots and numerical solution has been computed using MATLAB. The codes to obtain the results mentioned in this report can be accessed from this link - `https://drive.google.com/drive/folders/1fGQSdE08JU5VHLlmBvkjF3BBi29JCoj9?usp=share_link`.

REFERENCES

[1]K. Balasubramanian and R. Sujith, "Thermoacoustic instability in a rijke tube: Non-normality and nonlinearity," Physics of Fluids **20**, 044103 (2008).

[2]K. Manoj, S. A. Pawar, J. Kurths, and R. Sujith, "Rijke tube: A nonlinear oscillator," Chaos: An Interdisciplinary Journal of Nonlinear Science **32**, 072101 (2022).

[3]P. Subramanian, S. Mariappan, R. Sujith, and P. Wahi, "Bifurcation analysis of thermoacoustic instability in a horizontal rijke tube," International journal of spray and combustion dynamics **2**, 325–355 (2010).

[4]B. T. Zinn and M. E. Lores, "Application of the galerkin method in the solution of non-linear axial combustion instability problems in liquid rockets," Combustion Science and Technology **4**, 269–278 (1971).